

## Efficient and stable non-doped deep-blue organic light emitting diode based on an anthracene derivative

WANG ZhiQiang<sup>1,2</sup>, ZHENG CaiJun<sup>1</sup>, LIU Heng<sup>3</sup>,  
OU XueMei<sup>1</sup> & ZHANG XiaoHong<sup>1\*</sup>

<sup>1</sup>*Nano-organic Photoelectronic Laboratory and Key Laboratory of Photochemical Conversion and Optoelectronic Materials;  
Technical Institute of Physics and Chemistry, Chinese Academy of Sciences, Beijing 100190, China*

<sup>2</sup>*College of Chemistry and Chemical Engineering, Luoyang Normal University, Luoyang 471022, China  
Binzhou Polytechnic, Binzhou 256603, China*

Received November 26, 2010; accepted January 2, 2011

A new anthracene derivative 9,10-bis[3,5-di(4-*tert*-butylphenyl)phenyl]anthracene (BPPA) was synthesized via Suzuki coupling reaction and characterized by <sup>1</sup>H NMR spectrum, mass spectrum, and elemental analysis. BPPA exhibits deep-blue emission both in solution and in solid thin film. This compound has a non-planar structure that results in high thermal stability and the phenomenon of polymorphism. The non-doped device based on this material shows stable deep-blue emission with the 1931 Commission international de l'Eclairage (CIE) coordinate of (0.15, 0.05) under different applied voltages. The device exhibits the maximum external quantum efficiency of 2.2% at 14.9 mA/cm<sup>2</sup> with luminance of 105 cd/m<sup>2</sup>.

**organic light emitting diodes, anthracene derivative, deep-blue emission, theoretical calculations, thermal properties**

### 1 Introduction

Since the pioneering work on organic light emitting diodes (OLEDs) by the Kodak [1] and Cambridge groups [2], OLEDs have attracted considerable attention due to their potential application in flat panel displays. Three basic colors, red, green and blue, are essential for the full color OLEDs. During the past two decades, significant progress has been made in this field [3–6]. However, the performances of the blue-light-emitting OLEDs are still relatively poor in comparison with those of the red- and green-light-emitting OLEDs. Although the use of dopant emitters in the host-guest systems is an effective approach to improve the electroluminescence (EL) efficiency, the non-doped devices are more preferable for the purpose of the concise fabrication process. In addition to efficiency, color purity is an

other important essential for display applications. The 1931 CIE coordinate of blue emission specified in the National Television System Committee (NTSC) standard is (0.14, 0.08). In addition, it is well known that the power consumption of a full-color OLED is highly dependent upon the color of blue emission [7]. The deeper the blue color (smaller CIE y-value) is, the lower the power consumption of the device is. Recently, several deep-blue OLEDs with the 1931 CIE coordinates close to the NTSC standard have been reported [7–15], but the OLEDs with the coordinate of y<0.05 are still rare [16, 17].

Anthracene derivatives usually have a high fluorescence quantum yield, wide energy gap, and good thermal stability. Thus, they have been widely used as deep-blue emitting materials in OLEDs [7, 9, 15, 18–20]. In this paper, we report a novel anthracene derivative 9,10-bis[3,5-di(4-*tert*-butylphenyl)phenyl]anthracene (BPPA). The 3,5-di(4-*tert*-butylphenyl)phenyl groups end-capped at the 9- and 10-positions of the central anthracene core are highly twisted to

\*Corresponding author (email: xhzhang@mail.ipc.ac.cn)

increase steric hindrance and cause molecular non-planarity. This compound exhibits a high glass transition temperature ( $T_g$ ) and a phenomenon of polymorphism. The non-doped device based on BPPA shows stable deep-blue emission with the 1931 CIE coordinate of (0.15, 0.05) and high external quantum efficiency of 2.2%.

## 2 Experimental

Commercially available reagents were used without further purification unless otherwise stated.  $^1\text{H}$  NMR spectrum was recorded in  $\text{CDCl}_3$  solution on a Bruker Avance 400 spectrometer with tetramethylsilane (TMS) as the internal standard. Elemental analysis was performed on a Vario III elemental analyzer. Mass spectrum was obtained on a BIFLEXIII MALDI-TOF spectrometer. The UV absorption and photoluminescence spectra were recorded on a Hitachi U-3010 UV-vis spectrophotometer and a Hitachi F-4500 fluorescence spectrophotometer, respectively. With the heating rate of 10  $^\circ\text{C}/\text{min}$  under a nitrogen atmosphere, thermal gravimetric analysis (TGA) and differential scanning calorimetry (DSC) measurements were performed on a TA Instrument TGA2050 and a TA Instruments DSC2910, respectively. Cyclic voltammetry measurement was performed using a CHI600A analyzer with the scan rate of 500 mV/s in the  $\text{CH}_2\text{Cl}_2$  solution. The electrolytic cell was a conventional three-electrode cell in which a Pt disc working electrode, a Pt wire auxiliary electrode, and a saturated calomel electrode (SCE) as the reference electrode were employed. Tetra-*n*-butylammonium hexafluorophosphate (0.1 M) was used as the supporting electrolyte.

BPPA was synthesized via the Suzuki coupling reaction (Scheme 1). 3,5-Di(*tert*-butylphenyl)benzene boronic acid (**1**; 0.85 g, 2.2 mmol), 9,10-dibromoanthracene (**2**; 0.336 g, 1 mmol), tetrakis(triphenylphosphine)palladium [ $\text{Pd}(\text{PPh}_3)_4$ ] (20 mg), tetrahydrofuran (THF; 20 mL), and aqueous potassium carbonate (2 M, 5 mL) were sequentially added to a round bottom flask (50 mL). The resulting mixture was purged with nitrogen for 30 min, refluxed overnight, and poured into 100 mL water. The precipitate was filtered, washed several times with water, and dried. The crude

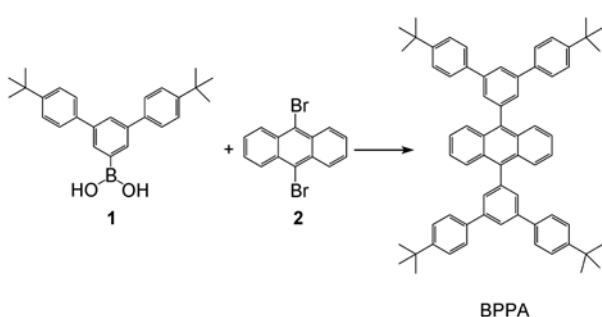
product was purified by column chromatography (eluent = dichloromethane/hexane, 1:10 v/v), and then recrystallized in toluene to give the product as a white solid (yield: 0.53 g, 62%).  $^1\text{H}$  NMR (400 MHz,  $\text{CDCl}_3$ )  $\delta$ (ppm): 7.87–8.04 (6H, m), 7.69–7.74 (12H, m), 7.50 (8H, d,  $J$  = 6.64), 7.34–7.38 (4H, m), 1.38 (36H, s); MALDI-TOF MS  $m/z$  59.3; Anal. calcd for  $\text{C}_{46}\text{H}_{34}$ : C, 92.26; H, 7.74; Found: C, 92.14; H, 7.78.

Indium-tin-oxide (ITO)-coated glass substrates with the sheet resistance of 50  $\Omega/\square$  were cleaned with isopropyl alcohol and deionized water, dried in an oven over 120  $^\circ\text{C}$ , and treated with UV-ozone. A 30 nm thick film of poly(3,4-ethylenedioxy thiophene) doped with poly(styrene sulfonate) (PEDOT:PSS) was spin-coated on the ITO glass substrates. After being dried at 120  $^\circ\text{C}$  for 30 min under the nitrogen atmosphere, the substrate was transferred to the vacuum deposition system with a base pressure of  $< 5 \times 10^{-7}$  torr. The device was fabricated by evaporating organic layers onto the PEDOT:PSS layer sequentially with an evaporation rate of 1–2 Å/s. After CsF layer was evaporated onto the organic layers, the Mg:Ag alloy cathode was prepared by co-evaporation of Mg and Ag at the volume ratio of 10:1. EL spectra and CIE color coordinates were measured with a spectrascan PR650 photometer and the current-voltage-luminescence characteristics were measured with a computer-controlled Keithley 2400 SourceMeter under ambient atmosphere.

## 3 Results and discussion

To gain insight into the electronic structure and the stereo-structure of BPPA, quantum chemical calculations were carried out using the B3LYP/6-31G(d) method [21]. The reliability of the method can be found in previous reports [22–24]. The aryl substituents at the 9- and 10- positions of the anthracene core are highly twisted toward the anthracene backbone with the torsion angle of 91.9°, which indicates that BPPA has a non-planar structure. The non-planarity of the structure can limit the intermolecular interactions, and facilitate the formation of stable amorphous film. The electron densities of the highest occupied molecular orbital (HOMO) and the lowest unoccupied molecular orbital (LUMO) are almost concentrated on the anthracene unit (Figure 1), suggesting that the absorption and emission of BPPA are controlled mostly by the central anthracene unit. Combining the half-wave oxidation potential ( $E_{1/2}^{\text{ox}}$ ) and the UV-vis absorption edge of BPPA, the HOMO and LUMO energy levels are estimated to be 5.91 and 2.89 eV, respectively.

The UV-vis absorption and photoluminescence (PL) spectra of BPPA in dilute  $\text{CH}_2\text{Cl}_2$  solution are shown in Figure 2. The absorption spectrum exhibits the characteristic vibration patterns of the isolated anthracene group at 336, 356, 375 and 397 nm [9, 10]. The strong absorption



**Scheme 1** Synthetic route of BPPA. Reagents and conditions: THF,  $\text{K}_2\text{CO}_3$ ,  $\text{Pd}(\text{PPh}_3)_4$ , reflux.

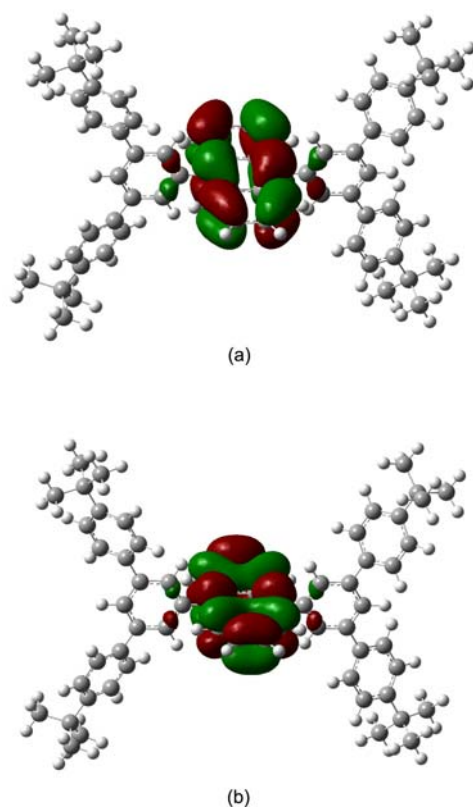


**Figure 1** Calculated HOMO (a) and LUMO (b) orbitals of BPPA.

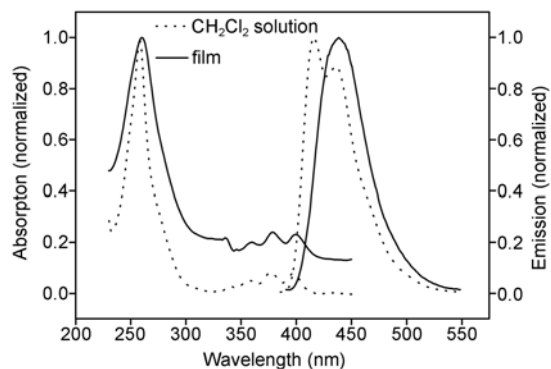


**Figure 2** The absorption and photoluminescence spectra of BPPA in dilute  $\text{CH}_2\text{Cl}_2$  solution (dotted line) and in solid film (solid line).

band at 260 nm can be assigned to the aryl groups at the 9- and 10-positions of the anthracene core. When BPPA is excited at 260 or 375 nm, the same PL spectra with  $\lambda_{\text{max}} = 415$  and 436 nm are observed, which indicates that the energy can be transferred from the side groups to the central anthracene unit. Fluorescence quantum yield ( $\Phi_f$ ) of BPPA in the dilute  $\text{CH}_2\text{Cl}_2$  solution has been measured to be 0.95 by using 9,10-diphenylanthracene ( $\Phi_f = 0.90$ ) as the calibration standard [25]. The absorption spectrum of BPPA as a solid thin film on a quartz disc is almost identical to that of BPPA in dilute  $\text{CH}_2\text{Cl}_2$  solution (Figure 2), which implies that the intermolecular interactions are very weak in the

solid film. The PL spectrum of the solid thin film shows a deep-blue emission with a structureless peak at 438 nm.

The thermal properties of BPPA were investigated through TGA and DSC under the nitrogen atmosphere. BPPA exhibits a high thermal stability, the decomposition temperature ( $T_d$ ), which corresponds to a 3% weight loss upon heating during TGA, is around 410 °C. DSC measurements were performed from 30 to 405 °C under the nitrogen atmosphere. Upon the first heating, an endothermic solid-solid phase transition was observed at 381 °C before the melting temperature ( $T_m$ ) of 391 °C (Figure 3). The melted sample was rapidly cooled by liquid nitrogen to form a glassy state. When the amorphous glassy sample was heated again, a glass transition occurred at 207 °C. The high glass transition temperature ( $T_g$ ) indicates that BPPA can form highly stable amorphous films. Upon further heating beyond  $T_g$ , an exothermic multi-peak due to crystallization was observed at around 320 °C, and then two endothermic solid-solid phase transition were observed at 377 and 381 °C, respectively, which indicates that BPPA has multiple crystal forms. The phenomenon of polymorphism suggests that BPPA has different conformers, which is responsible for the ready formation of the amorphous state.[26]

To investigate the EL properties of BPPA, we fabricated the non-doped device with a configuration of ITO/PEDOT: PSS (30 nm)/NPB (15 nm)/TCTA (15 nm)/BPPA (30 nm)/TPBI (30 nm)/CsF (2 nm)/Mg:Ag. In this device, ITO and CsF/Mg:Ag are the anode and the cathode, respectively; PEDOT:PSS is the hole-injection layer (HIL); 4,4'-bis[N-(1-naphthyl)-N-phenyl amino] biphenyl (NPB) is the hole-transporting layer (HTL); 4,4',4''-tri(N-carbazolyl)triphenylamine (TCTA) is used as the hole-transporting and electron-blocking layer (HT-EBL); 1,3,5-tris(*N*-phenylbenzimidazol) benzene (TPBI) is used as the electron-transporting layer and hole-blocking layer (ET-HBL); BPPA is the emitting layer (EML).

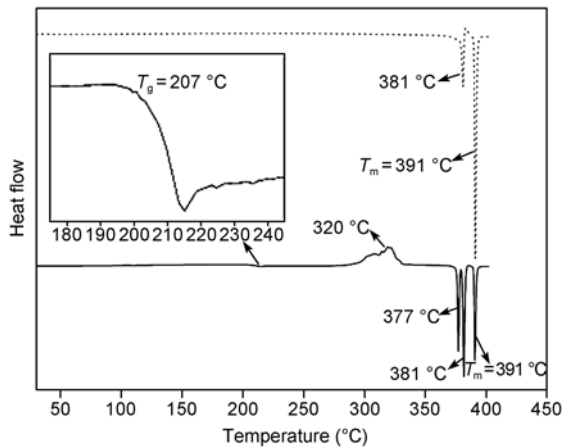


**Figure 3** The DSC curves of BPPA (dotted line for the first heating of the original sample, solid line for the second heating of the amorphous glassy sample).

Figure 4 shows the normalized EL spectra of the device at different applied voltages. All the emission peaks are at 430 nm with very narrow FWHM (the full width at half maximum) of about 55 nm. The EL spectra show no emission in the longer wavelength region which is often observed in the case of intermolecular  $\pi$ - $\pi$  stacking or charge-transfer complexes formed at the EML/HTL or EML/ETL interface. The high quality emission should be attributed to the non-planar structure of BPPA. While increasing the applied voltage from 5 to 10 V, the EL spectra remain unchanged, which is desirable for OLEDs. The 1931 CIE coordinate (0.15, 0.05) of this device is far beyond the NTSC blue standard, which may provide an enlarged color gamut for color displays. Up to now, the devices with CIE coordinates of  $y < 0.05$  are still very rare to our knowledge [16, 17].

Schematic energy level diagram of the BPPA based device is shown in Figure 5. It can be seen that the hole-injection barrier at the TCTA/BPPA interface and the electron-injection barrier at the BPPA/TPBI interface is 0.21 and 0.09 eV, respectively. These small carrier-injection barriers indicate that both holes and electrons could be readily injected into the emitting layer. In addition, from the energy level diagrams, it is also obvious that there are large hole-injection

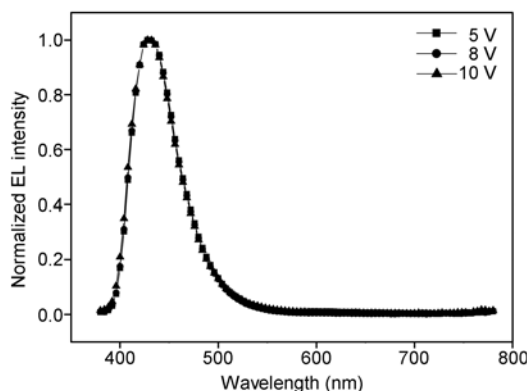


Figure 4 The EL spectra of the BPPA based device at different applied voltages.

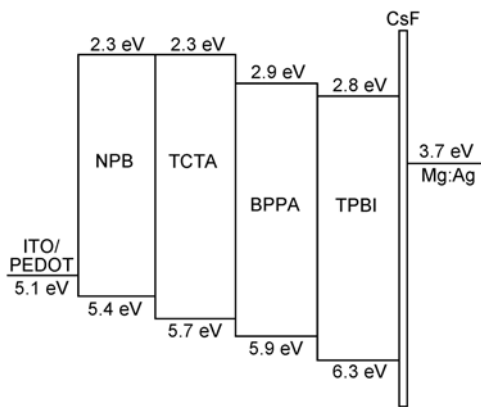


Figure 5 Relative energy level alignments of the BPPA based device.

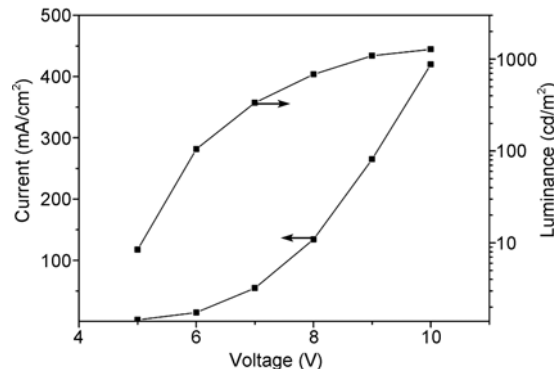


Figure 6 The current density-voltage-luminance characteristics of the BPPA based device.

barrier (0.39 eV) at the BPPA/TPBI interface and large electro-injection barrier (0.59 eV) at the TCTA/BPPA interface, which should efficiently prevent both holes and electrons leaving the emitting layer. Figure 6 shows the current density-voltage-luminance characteristics of the device. The turn-on voltage is 4.3 V, and the maximum luminance is 1280 cd/m<sup>2</sup> at the voltage of 10 V and the current density of 420 mA/cm<sup>2</sup>. The device exhibits the maximum external quantum efficiency of 2.2% (current efficiency of 0.7 cd/A) at 14.9 mA/cm<sup>2</sup> with the luminance of 105 cd/m<sup>2</sup>.

#### 4 Conclusion

A highly efficient deep-blue anthracene derivative BPPA was synthesized. This compound has a high thermal stability ( $T_d = 410$  °C and  $T_g = 207$  °C), and exhibits the phenomenon of polymorphism, which implies that it can form the stable amorphous thin film readily. The non-doped device based on this material shows stable deep-blue emission at 430 nm under different applied voltages. A maximum external quantum efficiency of 2.2% was achieved at 14.9 mA/cm<sup>2</sup> with the luminance of 105 cd/m<sup>2</sup>. The 1931 CIE coordinate (0.15, 0.05) of this device is far beyond the NTSC blue standard, which may provide an enlarged color gamut for color displays.

This work was supported by the National Natural Science Foundation of China (50773090, 50825304, 51033007).

- 1 Tang CW, Vanslyke SA. Organic electroluminescence diode. *Appl Phys Lett*, 1987, 51: 913–915
- 2 Burroughes JH, Bradley DDC, Broun AR, Marks RN, Mackay K, Friend RH, Burn PL, Holmes AB. Light-emitting diodes based on conjugated polymers. *Nature*, 1990, 347: 539–541
- 3 Tang CW, Vanslyke SA, Chen CH. Electroluminescence of doped organic thin films. *J Appl Phys*, 1989, 65: 3610–3616
- 4 Shi J, Tang CW. Doped organic electroluminescent devices with improved stability. *Appl Phys Lett*, 1997, 70: 1665–1667
- 5 Baldo MA, O'Brien DF, You Y, Shoustikov A, Sibley S, Thompson

- ME, Forrest SR. Highly efficient phosphorescent emission from organic electroluminescent devices. *Nature*, 1998, 395: 151–154
- 6 Sun Y, Giebink NC, Kanno H, Ma B, Thompson ME, Forrest SR. Management of singlet and triplet excitons for efficient white organic light-emitting devices. *Nature*, 2006, 440: 908–912
  - 7 Zheng CJ, Zhao WM, Wang ZQ, Huang D, Ye J, Zhang XH, Lee CS, Lee ST. Highly efficient non-doped deep-blue organic light-emitting diodes based on anthracene derivatives. *J Mater Chem*, 2010, 20: 1560–1566
  - 8 Wang L, Jiang Y, Wang J, Pei J, Cao Y. Highly efficient and color-stable deep-blue organic light-emitting diodes based on a solution-processible dendrimer. *Adv Mater*, 2009, 21: 4854–4858
  - 9 Chien CH, Chen CK, Hsu FM, Shu CF, Chou PT, Lai CH. Multifunctional deep-blue emitter comprising an anthracene core and terminal triphenylphosphine oxide groups. *Adv Funct Mater*, 2009, 19: 560–566
  - 10 Shih PI, Chuang CY, Chien CH, Shu CF.. Highly efficient non-doped blue-light-emitting diodes based on an anthracene derivative end-capped with tetraphenylethylene groups. *Adv Funct Mater*, 2007, 17: 3141–3146
  - 11 Gao Q, Li ZH, Xia PF, Wong MS. Efficient deep-blue organic light-emitting diodes: Arylamine-substituted oligofluorenes. *Adv Funct Mater*, 2007, 17: 3194–3199
  - 12 Moorthy JN, Venkatakrishnan P, Huang DF, Chow TJ. Blue light-emitting and hole-transporting amorphous molecular materials based on diarylaminobiphenyl-functionalized bimesitylenes. *Chem Commun*, 2008, 2146–2148
  - 13 Zhen CG, Chen ZK, Liu QD, Kieffer J. Fluorene-based oligomers for highly efficient and stable organic blue-light-emitting diodes. *Adv Mater*, 2009, 21: 2425–2429
  - 14 Liao SH, Shiu JR, Liu SW, Yeh SJ, Chen YH, Chen CT, Chow TJ, Wu CI. Hydroxynaphthyridine-derived group III metal chelates: Wide band gap and deep blue analogues of green Alq<sub>3</sub> (tri(8-hydroxyquinolate) aluminum) and their versatile applications for organic light-emitting diodes. *J Am Chem Soc*, 2009, 131: 763–777
  - 15 Kim YH, Shin DC, Kim SH, Ko CH, Yu HS, Kwon SK. Novel blue emitting material with high color purity. *Adv Mater*, 2001, 13: 1690–1693
  - 16 Wu CC, Lin YT, Wong KT, Chen RT, Chien YY. Efficient organic blue-light-emitting devices with double confinement on terfluorenes with ambipolar carrier transport properties. *Adv Mater*, 2004, 16: 61–65
  - 17 Tang S, Liu MR, Lu P, Xia H, Li M, Xie ZQ, Shen FZ, Gu C, Wang HP, Yang B, Ma YG. A molecular glass for deep-blue organic light-emitting diodes comprising a 9,9'-spirobifluorene core and peripheral carbazole groups. *Adv Funct Mater*, 2007, 17: 2869–2877
  - 18 Tao SL, Hong ZR, Peng ZK, Ju WG, Zhang XH, Wang PF, Wu SK, Lee ST. Anthracene derivative for a non-doped blue-emitting organic electroluminescence device with both excellent color purity and high efficiency. *Chem Phys Lett*, 2004, 397: 1–4
  - 19 Kim YH, Jeong HC, Kim SH, Yang K, Kwon SK. High-purity-blue and high efficiency electroluminescent devices based on anthracene. *Adv Funct Mater*, 2005, 15: 1799–1805
  - 20 Kim SK, Yang B, Ma YG, Lee JH, Park JW. Exceedingly efficient deep-blue electroluminescence from new anthracenes obtained using rational molecular design. *J Mater Chem*, 2008, 18: 3376–3384
  - 21 Frisch MJ, Trucks GW, Schlegel HB, Scuseria GE, Robb MA, Cheeseman JR. Gaussian 03, Revision A1, Gaussian Inc, Pittsburgh, PA 2003
  - 22 Lee SJ, Park JS, Yoon KJ, Kim YI, Jin SH, Kang SK. High-efficiency deep-blue light-emitting diodes based on phenylquinoline/caybazole-based compounds. *Adv Funct Mater*, 2008, 18: 3922–3930
  - 23 Wang ZQ, Xu C, Wang WZ, Fu WJ, Niu LB, Ji BM. Highly efficient undoped deep-blue electroluminescent device based on a novel pyrene derivative. *Solid-State Electron*, 2010, 54: 524–526
  - 24 Liu F, Tang C, Chen QQ, Li SZ, Wu HB, Xie LH. Pyrene functioned diarylfluorenes as efficient solution processable light emitting molecular glass. *Org Electron*, 2009, 10: 256–265
  - 25 K. Danel, T. H. Huang, J. T. Lin, Y. T. Tao, C. H. Chuen. Blue-emitting anthracenes with end-capping diarylamines. *Chem Mater*, 2002, 14: 3860–3865
  - 26 Shirota Y. Organic materials for electronic and optoelectronic devices. *J Mater Chem*, 2000, 10: 1–25